Some features of anisothermal solid-state transformations in alloy 718

Aliou Niang, Bernard Viguier, Jacques Lacaze

Some features of anisothermal solid-state transformations in alloy 718

*Aliou Niang, Bernard Viguier, Jacques Lacaze**

CIRIMAT, Université de Toulouse, 31077 Toulouse cedex 4, France

A B S T R A C T

This paper presents an attempt to use differential thermal analysis to study anisothermal precipitation of both the stable delta and the metastable gamma-second phases during cooling of alloy Inconel 718. Observation of the samples by scanning and transmission electron microscopy was carried out to identify the thermal arrests observed upon cooling. When the upper temperature of the cycle is above the solvus of the delta phase, a clear peak is observed that could be related to precipitation of gamma-second for all the cooling rates used in the present work. When this temperature is below the delta solvus, no thermal arrest can be observed, while when it is close to it two faint peaks were noted and associated with stable and metastable precipitation. The most striking result was that dissolution of the metastable gamma-second phase during the heating stage was found to proceed heterogeneously in the material, and this affected reprecipitation of the phases upon subsequent cooling.

Keywords:
Differential thermal analysis
Inconel 718
Ni_3Nb precipitation
Delta phase
γ'' phase
Transmission electron microscopy

1. Introduction

The phases that are responsible for high mechanical properties of alloy 718 are the γ'', $D0_{22}$ ordered Ni_3Nb phase, and to a lesser extent the γ', $L1_2$ $Ni_3(Al,Ti)$ phase [1]. The γ'' phase is metastable with respect to the orthorhombic $D0_a$ Ni_3Nb phase denoted δ [1,2]. As mentioned by Oradei-Basile and Radavich [3], the only carbides that can be found in modern 718 alloy are of the MC type thanks to the use of vacuum casting and the associated decrease in the carbon content with respect to older production. These carbides precipitate at high temperature and are stable in the usual forming range as long as the temperature is not brought to 1200 °C where they may partly dissolve. Forging is performed at temperatures varying around 1000 °C at which some dispersed precipitates of δ phase limit grain growth. The semi-finished parts are then hardened by means of isothermal heat-treatments at much lower temperatures where only the γ' and γ'' phases precipitate.

Brooks and Bridge [4] and Oradei-Basile and Radavich [3] have drawn transformation–time–temperature (TTT) diagrams for precipitation of γ' and γ''. These authors stressed the fact that the precipitates are too small at the early stage of precipitation to be easily identified. Accordingly, Oradei-Basile and Radavich [3] drew one single precipitation curve for both phases, and this corresponds to the observations by Han et al. [5]. On the contrary, Brooks and Bridge [4] found that γ'' first precipitates alone, the γ' phase appearing at much longer times. This appears to contradict other results, e.g. those from Marsh who reported that γ' appears before γ'' during isothermal ageing between 780 and 820 °C [6], or from Slama and Abdellaoui [7] for ageing at 680 °C. Sundararaman et al. [8] reported that they could not ascertain which of the phases formed first, except for ageing at 900 °C where they observed

* *Corresponding author*. Tel.: +33 562 88 5710; fax: +33 562 88 5663.
E-mail address: jacques.lacaze@ensiacet.fr (J. Lacaze).

doi:10.1016/j.matchar.2010.02.011

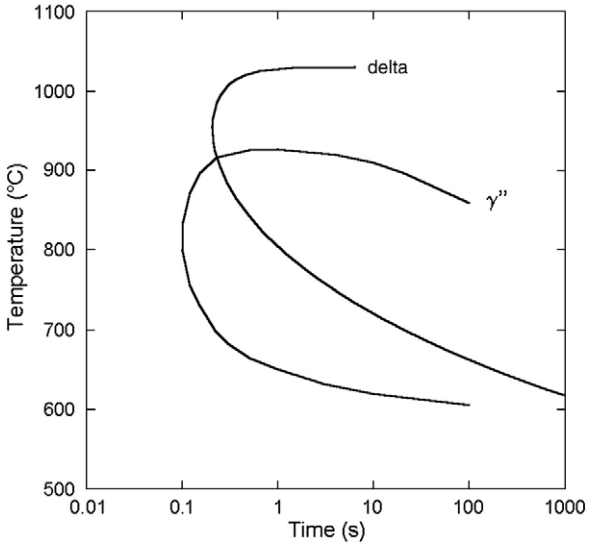

Fig. 1 – TTT curves for δ and (γ′+γ″) precipitation.

only the γ'' phase, concluding this latter phase should have a metastable solvus higher than that of the γ' phase. Also, Brooks and Bridge [4] observed precipitation at 700 °C at much shorter times than reported by Oradei-Basile and Radavich [3], in agreement with other works [7]. Because of the uncertainties stressed above, we considered, for the present study, that the curve for precipitation of γ'' given by Brooks and Bridge [4] could be used to describe the domain for isothermal precipitation of either or both of the γ' and γ'' phases. This curve has been is plotted in Fig. 1 where the curve for the onset of δ precipitation as assessed in a previous work is also reproduced [9]. The two curves appear to cross each other at about 920 °C, not far from the 900 °C proposed by Sundararaman et al. [10].

According to Fig. 1, the δ phase is expected to precipitate and grow upon slow cooling from high temperature, while at intermediate and high cooling rates the metastable γ'' should be favoured. The γ' phase is a stable phase in alloy 718, and should appear in most cases. At very high cooling rates however, no precipitate will form and the matrix gets supersaturated in alloying elements, in particular niobium. Though highly relevant for practical purposes, very few studies have looked at the effect of cooling rate on precipitation kinetics in the temperature range relevant for forging. A few CCT curves were drawn [11–14] that will be described further in the Discussion section. The present work was aimed at defining the capabilities of differential thermal analysis experiments to support a study on investigating phase transformations involving δ and γ'' phases at intermediate heating or cooling rates relevant to forging operations.

2. Experimental Details

The material used for this study has been was provided by Aubert & Duval as a 200 mm piece of a bar 178 mm in diameter. This bar had been forged from a vacuum induction melting plus vacuum arc remelting (VIM–VAR) processed ingot that was 50.8 cm in diameter. After ageing, the bar had then been submitted to an annealing treatment at 968 °C for 1 h and to precipitation treatments at 720 °C (8 h) and 620 °C (8 h), and was finally air cooled to room temperature (RT). A chemical analysis was performed (at the CNRS Central Analysis Service) by induction coupled plasma–atomic emission spectroscopy (ICP–AES) for metallic elements and by combustion and infrared spectroscopy for carbon. The results are given in Table 1 where the composition obtained may be compared to the nominal one.

For metallographic observations, sections of the material or samples were mechanically polished down to 3 μm diamond paste. The final preparation consisted either in a polishing with OPS® suspension or an electro-chemical etching with oxalic acid for grain boundary observations or phosphoric and sulphuric acids to reveal the δ phase. Observations were performed on an Olympus PMG3 optical microscope (OM) and a LEO 435 VP scanning electron microscope (SEM). SEM images were obtained using either secondary (SE detector) or back scattered electrons (QBSD detector) depending on the information required. Typical microstructure of the material in the as-received (referred to as AR in this paper) state is shown in Fig. 2. The OM micrograph in Fig. 2-A shows that the material underwent a partial recrystallisation and more detailed observation reveals the presence of some intergranular δ precipitates that appear in light contrast in Fig. 2-B.

Differential thermal analyses (DTA) were performed using a Setsys apparatus from SETARAM. Samples were small pieces weighing 0.25 to 0.35 g; they were all taken out at mid-radius of the bar. The solvus of the alloy was first investigated through the heating, at various rates, of samples machined out from a specimen that had been water quenched after a 10 h heat treatment at 900 °C to have copious precipitation of the δ phase as shown in a previous study [9]. This material will be labelled HT throughout this paper.

All other DTA experiments were performed on AR material to study precipitation during cooling. In order to limit the formation of the δ phase as much as possible when heating the material, a heating rate of 30 °C/min was adopted for all experiments. Various attempts were performed to look at the

Table 1 – Chemical composition of the alloy studied in the present work and nominal composition of alloy 718 [22].

	Ni	Fe	Cr	Nb	Mo	Co	Al	C	Si (ppm)	Mn (ppm)
Present study (at. %)	54.47	18.27	20.07	3.39	1.9	0.21	1.08	0.5	2369	743
Present study (wt. %)	52.95	17.09	17.49	5.28	3.05	0.21	0.49	0.12	1116	684
Nominal composition (wt. %)	52.50	18.50	19.00	5.10	3.00	–	0.50	0.08	–	–

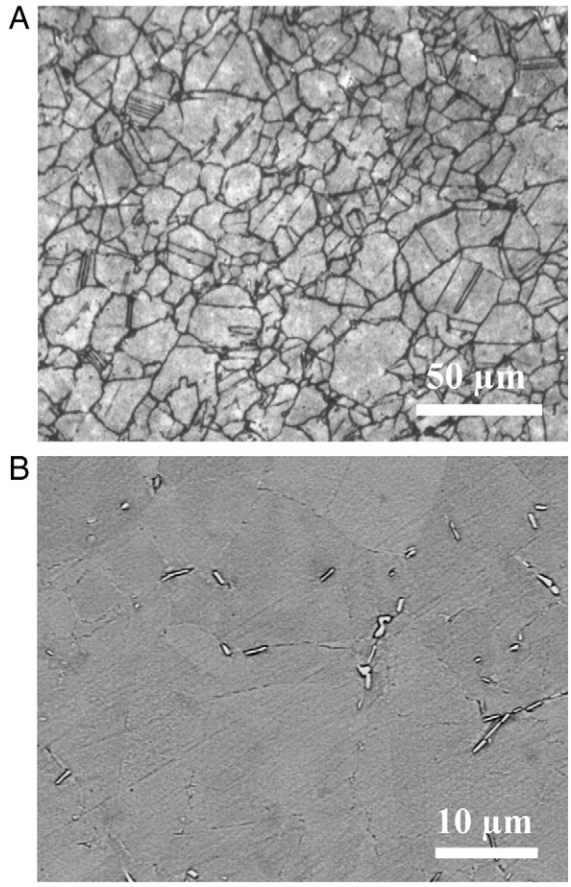

Fig. 2 – Microstructure of the material in the as-received condition as observed by optical microscopy (OM) (A) and by scanning electron microscopy (SEM) with the QBSD detector (B).

effect of the upper temperature, of the holding time at that temperature and of the cooling rate on the transformations occurring during subsequent cooling. The whole set of DTA experiments performed in this study is listed in Table 2.

Preparation of the foils for transmission electron microscopy (TEM) observations were classically conducted by cutting slices that were mechanically ground down to a thickness of about 80 µm. Final thinning was performed in a Struers twin-jet Tenupol-5® using an electrolyte containing 900 ml of methanol, 100 ml of perchloric acid and 200 ml of Butylcellosolve. The operation was performed at a temperature below 0 °C, usually between −5 and −10 °C, under a potential of 22 V. A Jeol 2010 transmission electron microscope, from the TEMSCAN service of Paul Sabatier University, was used under 200 kV.

3. Results

3.1. DTA Records Upon Heating

The first series of heating experiments was performed on HT materials to evaluate the solvus temperature of the δ phase. Fig. 3 shows the microstructure of the material after heat treating for 10 h at 900 °C and then quenching to RT. Copious

Table 2 – Listing of the DTA experiments indicating the initial state of each sample (HT for heat-treated 10 h at 900 °C, AR for as received), heating and cooling rates, and holding time at the high temperature of the DTA cycle.

Initial state of the sample	$V_{heating}$ (°C/min)	Maximum temperature (°C)	Holding time (s)	$V_{cooling}$ (°C/min)
HT	10	1150	1	10
	20	1150	1	10
	5	1150	1	10
AR	30	980	36000	5
	30	980	1800	5
	30	1100	600	10
	30	1100	1	10
	30	1100	600	10
	30	1100	1200	10
	30	1100	1800	10
	30	980	1	10
	30	940	1	10
	30	1020	1	10
	30	1060	1	10
	30	1020	1	5
	30	1020	1	20
	30	1000	1	10
	30	980	600	10

precipitation was observed which presents the characteristic features of the δ phase, i.e. intergranular, discontinuous precipitates and thin, intragranular plates [2,3,8–10]. According to previous results [9], the volume fraction of the δ phase precipitated during this treatment should be slightly lower than the equilibrium value that was evaluated at 8% [15]. Note that this latter value is significantly lower than the predicted 13% equilibrium value at room temperature [15], so that the matrix of the HT material after quenching to RT should be supersaturated in niobium as significant precipitation of δ or of γ' and γ'' phases is not expected to take place during this rapid cooling.

Fig. 4 shows the DTA records obtained while heating the HT material at 5, 10 and 20 °C/min up to 1150 °C, i.e. a temperature at which the material should be single phase (apart for the possible presence of a few carbides). The records show similar features at all three heating rates with peaks that get higher as the heating rate is increased. Because of the remaining matrix supersaturation mentioned above, it is expected that γ' and γ''

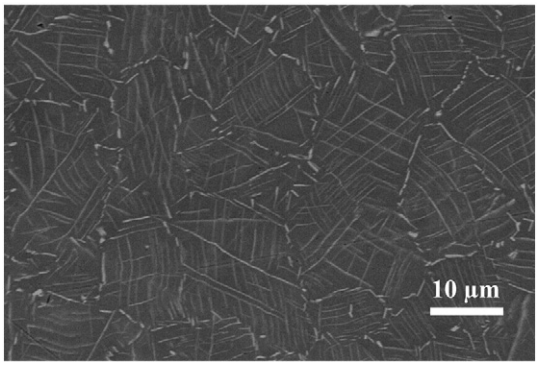

Fig. 3 – SEM micrograph (QBSD detector) of the structure after isothermal holding at 900 °C for 10 h and water quenching.

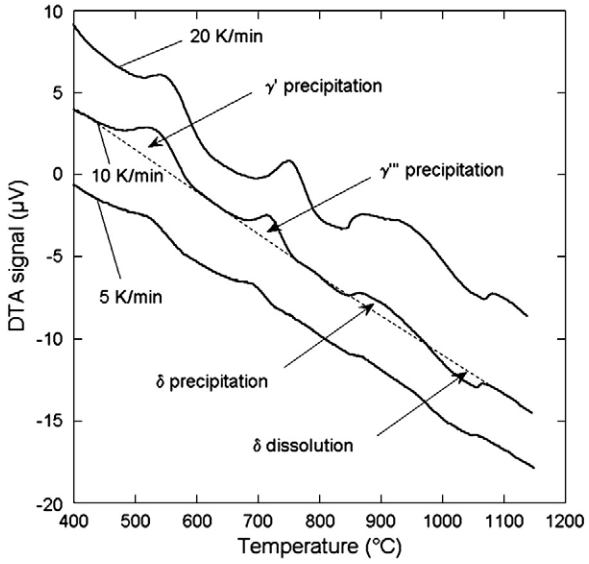

Fig. 4 – DTA records obtained on the heat-treated material (10 h at 900 °C, water quenching) upon heating at scanning rates of 5, 10 and 20 °C/min.

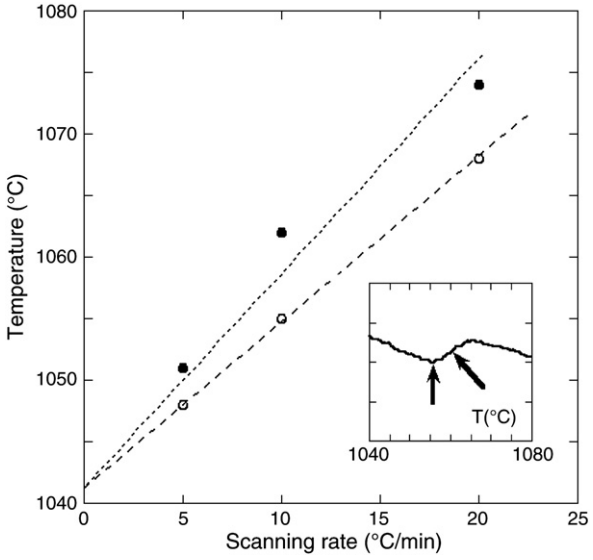

Fig. 5 – Determination of the δ solvus temperature by extrapolation to a zero scanning rate of the temperatures characterizing the peak of δ dissolution (the insert exemplifies how these temperatures were determined on the 10 °C/min curve).

precipitation may occur during heating. Based on the previous analysis by Slama et al. [16], the two exothermic peaks at 500 °C and 700 °C have been indexed as precipitation of γ' and of γ'' respectively. As the temperature is further increased, a third exothermic peak at 850 °C and an endothermic peak above 1000 °C are observed. They have been assigned to the transformation of γ'' to δ and finally dissolution of δ. This proposal is indicated in Fig. 4 where it appears to be supported by the drawing of a tentative base line (dotted curve) alongside the record obtained at the intermediate heating rate.

Two temperatures were measured on the DTA traces as being characteristic of the δ solvus: i) the temperature at the minimum of the peak related to δ dissolution; and ii) the temperature at the inflexion point on the return of the signal to the base line — these two points are shown in the insert in Fig. 5 which corresponds to the 10 °C/min curve of Fig. 4. These temperatures have been plotted versus the heating rate in Fig. 5. Though the temperatures at the inflexion point appear more scattered, both sets of values could be extrapolated to the same temperature on the y axis that is supposed to represent the equilibrium solvus of the δ phase. This solvus temperature is found to be 1041 °C.

All other DTA experiments were performed on AR material to study precipitation during cooling, although the heating stage will be considered first as it allows checking reproducibility. As seen in Table 2, five experiments had an upper temperature of 1100 °C and all showed highly similar DTA records, one of them being plotted with a bold line at the bottom of Fig. 6. Because of the increased heating rate, it proved more difficult to define a base line than was the case for the records shown in Fig. 4. However, the traces show various arrests that were tentatively indexed with arrows in the figure: i) a limited precipitation of γ' with a peak temperature at 550 °C; ii) a precipitation of γ'' with a peak temperature at about 750 °C, though spread over a much larger temperature range than for the HT material; iii) a faint slope change that could relate to precipitation of δ phase; and, finally, iv) an endothermic peak. The latter should be associated with dissolution of a phase, and it is worth stressing that it appears at a much lower temperature than the one in Fig. 4. Because of this lower temperature and because there is very few delta phase in the AR material, it is suggested that this peak may be related to the dissolution of the γ'' phase and not to the δ phase as previously.

Other similar experiments were performed at a heating rate of 30 °C/min with a maximum temperature set at 940, 980, 1020 and 1060 °C. One record from each series, i.e. one record for each maximum temperature, has been plotted in Fig. 6. All

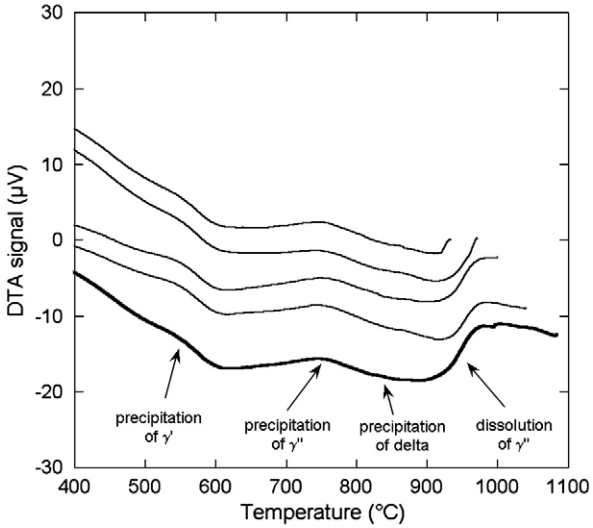

Fig. 6 – Comparison of the DTA records during heating of the as-received material at 30 °C/min up to various temperatures: 940, 980, 1020, 1060 and 1100 °C. The traces have been shifted along the y axis for clarity.

records present the same features, the only difference being the extent of the thermal arrest associated with the dissolution of the γ'' phase as the highest temperature of the cycle is decreased. The amplitude of this arrest is similar for the records with an upper temperature at 1020, 1060 and 1100 °C, while it appears significantly smaller for the records with an upper temperature at 940 °C and 980 °C. This means that the dissolution of γ'' was certainly not completed at the end of the heating stage in these two latter cases although the solvus of this phase should be in the range 900 to 920 °C according to the review presented in the introduction.

3.2. *DTA Records Upon Cooling*

The DTA cycles of the series of experiments with an upper temperature at 1100 °C differed by the holding time at that temperature, which was increased from 1 to 1800 s, while the cooling rate was still set at 10 °C/min (see Table 2). Whatever the duration of this holding, the DTA traces obtained upon cooling showed the same features characterized by one single precipitation peak with a maximum at about 780 °C. This peak is indicated with a double arrow on the bottom trace in Fig. 7; it is very similar to the peak observed by Slama and Cizeron with the same technique [16]. In many cases, a bounce of the DTA trace was observed when the signal reached the base line shortly after the cooling had started. This bounce is indicated with a solid arrow in the figure; it is understood to be an oscillation due to a non-steady thermal effect in the establishment of the base line when changing from a holding to a cooling regime.

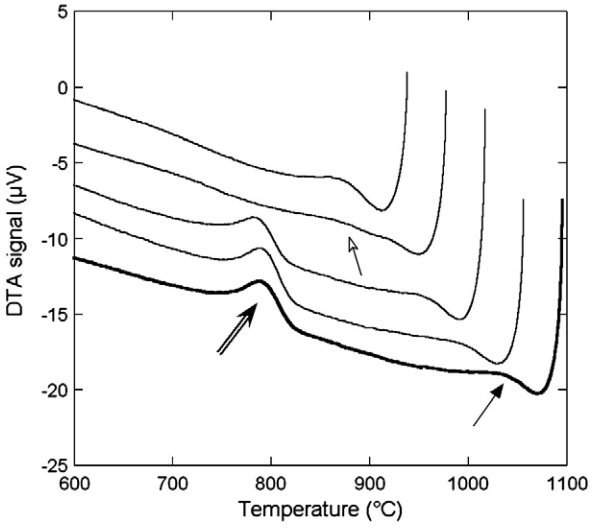

Fig. 7 – DTA traces obtained on cooling with the samples heated to 940, 980, 1020, 1060 and 1100 °C. The double arrow shows the peak at about 780 °C observed on DTA traces recorded upon cooling of material heated up to a temperature equal to or higher than 1000 °C. The solid arrow illustrates the bounce that was most often observed on the DTA traces when the signal reached its new baseline at the beginning of cooling. The open arrow indicates a slight slope change on the record obtained from the sample cooled from 980 °C. The traces have been shifted along the y axis for clarity.

Fig. 8-A shows a SEM micrograph of the sample held 1 s at 1100 °C and then cooled down to RT at 10 °C/min, that is representative of the whole series of samples cooled from 1100 °C. The blocky precipitates in light contrast are carbides, and the alloy did not seem to undergo any precipitation of the δ phase upon cooling. This suggests that the thermal arrest observed on the bottom record in Fig. 7 relates to γ'' precipitation. This was confirmed by TEM analysis as shown by the dark field micrograph in Fig. 8-B that was obtained from a $1\frac{1}{2}0$ spot along the $[001]_\gamma$ zone axis. Copious precipitation of γ'' was observed with precipitates that appear evenly distributed, showing a slightly elliptic shape 30 nm long and 20 nm thick.

Fig. 7 also shows the DTA records obtained upon cooling the samples at 10 °C/min held 1 s at the various maximum temperatures investigated, corresponding to the set of heating records in Fig. 6. For a starting temperature equal to or higher than 1020 °C, cooling at 10 °C/min leads to the same single peak as described above, with a maximum at about 780 °C, that was related to the precipitation of γ''. On the contrary, when the highest temperature of the cycle is 940 °C, no precipitation showed up on the DTA trace. Finally, a close examination of the DTA record obtained upon cooling from

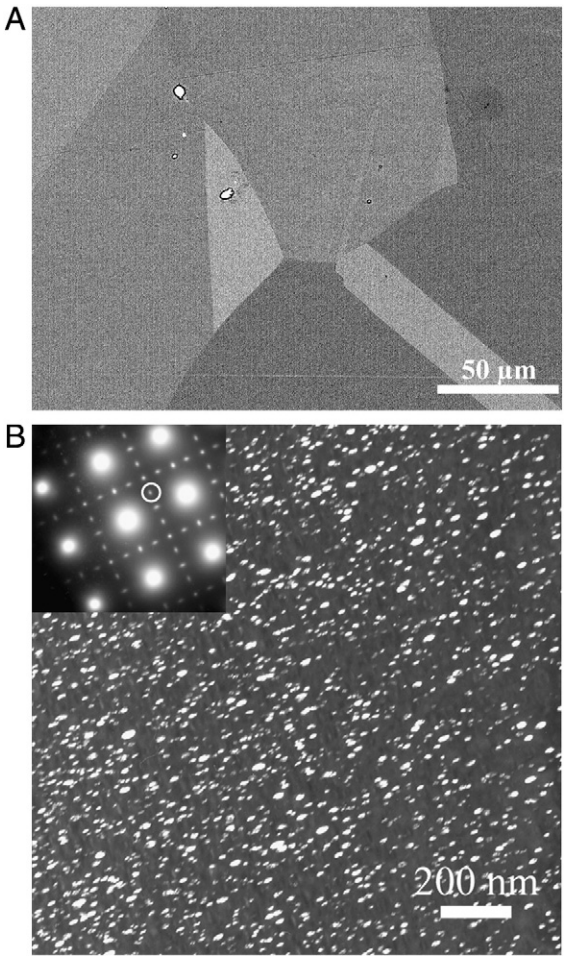

Fig. 8 – SEM (SE detector) (A) and TEM dark field (B) micrographs of the sample hold 1 s at 1100 °C and then cooled to RT at 10 °C/min.

980 °C reveals a faint slope change at about 910 to 920 °C with a shallow peak at 850 °C. This peak is marked with an open arrow in the figure, and it will be discussed further later.

SEM observation of the samples heated to a maximum temperature equal to 940, 980 and 1020 °C, and then cooled to RT, all showed the presence of some δ phase precipitates, mainly at grain boundaries. It was difficult to determine if these precipitates were residual δ phase remaining at the end of the heating stage, or if they developed during cooling. Two additional trials were thus performed with heating to 1020 °C at 30 °C/min, holding 1 s and then cooling at 5 and 20 °C/min respectively. The micrograph in Fig. 9-B shows that the amount of δ phase is slightly lower after cooling at 20 °C/min than after cooling at 5 °C/min (Fig. 9-A). It may thus be concluded that most of the δ phase observed in the sample cooled at 10 °C/min from 1020 °C did, in fact, precipitate during cooling. Because no δ phase appeared during cooling from higher temperatures, it may also be stated that this growth needs some remaining δ precipitates. In other words, the δ phase can grow when pre-existing, but does not nucleate for the cooling conditions imposed in the present study. Similarly, it seems reasonable to assume that some δ phase did also grow during the cooling stage from 940 or 980 °C. Unfortunately, this growth could be only evidenced on the DTA record for material cooled from 980 °C by the thermal arrest at about 850 °C pointed out with an open arrow in Fig. 7.

TEM study of the sample heated up to 1020 °C and then cooled at 10 °C/min showed the same distribution of γ'' precipitates as the one shown in Fig. 8-B. On the contrary, the TEM micrograph in Fig. 10 shows sparse and coarse γ'' precipitates in the sample that was heated up to 980 °C. According to the above observations on the DTA records, this difference may be related to the presence or absence of the peak at 850 °C upon cooling. This suggests that the dissolution of the γ'' precipitates above the solvus of this phase during the heating stage of the DTA is slow enough for some of them to remain and even coarsen during the upper part of the cycle up to 980 °C. This leads to a low supersaturation of the matrix when cooling down so that no γ'' reprecipitation occurs. On the contrary, heating up to 1020 °C ensures full dissolution of the precipitates and thus a higher supersaturation of the matrix that will lead to ample nucleation and fine γ'' precipitation upon cooling. This interpretation was verified by checking the number and size of precipitates in the samples heated to 940 °C and 1060 °C that were found to be similar to the ones heated to 980 °C and 1020 °C respectively.

The results of the systematic experiments presented above suggested performing two additional trials, firstly repeat heating to 980 °C but with holding at temperature before cooling (10 min), and secondly selecting 1000 °C as the target temperature. The DTA records obtained upon cooling during these additional experiments are compared in Fig. 11 with the record on the sample held 1 s at 980 °C. The bounce due to non-steady conditions (solid arrow) is more or less pronounced in these three curves. The faint slope change that was mentioned in relation to Fig. 7 appears as a clear thermal arrest with a peak at 850 °C after limited holding at 980 °C or if the target temperature is raised to 1000 °C (open arrow). This arrest occurs at a definitely higher temperature than the precipitation peak at 780 °C observed previously (Fig. 7) that

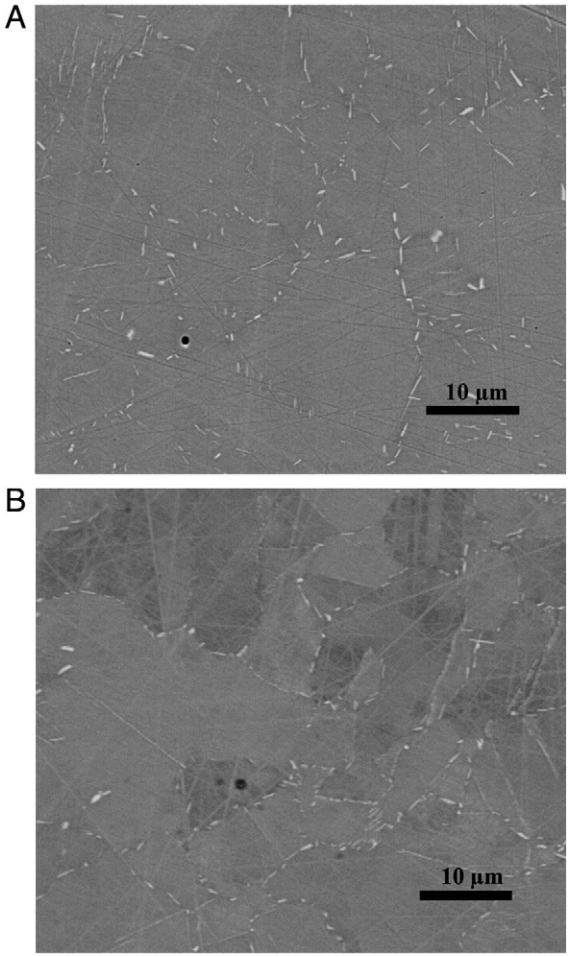

Fig. 9 – SEM images (QBSD detector) of samples heated to 1020 °C, then cooled at 5 °C/min (A) and 20 °C/min (B).

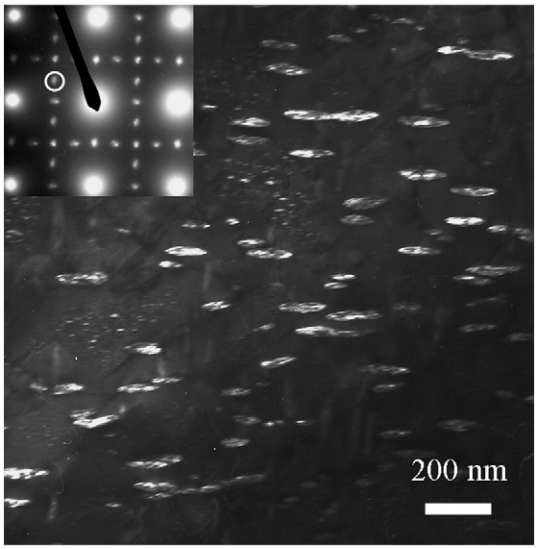

Fig. 10 – TEM dark field images of the samples heated up to 980 °C, held 1 s and cooled at 10 K/min.

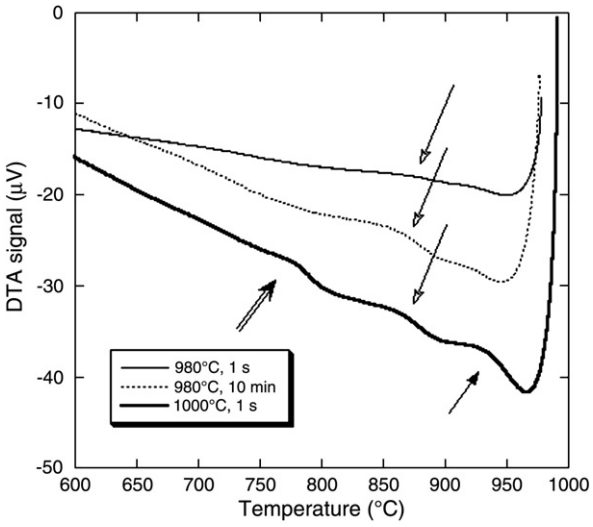

Fig. 11 – Comparison of the DTA records obtained upon cooling at 10 °C/min from 980 °C after 1 s or 600 s holding at temperature, and from 1000 °C after 1 s holding. The arrows have the same meaning as in Fig. 7.

had been associated with γ'' precipitation. Fig. 12 compares the SEM images of the samples heated to 980 °C and held at that temperature for 1 s (Fig. 12-A) and 10 min (Fig. 12-B) that show very similar δ phase precipitation though slightly more intragranular precipitation seems to have occurred in the latter case. While some δ phases could have precipitated during holding, ample precipitation of this phase occurred during cooling and was associated with a peak at 850 °C.

Fig. 11 also shows that, in the case of cooling from 1000 °C, the peak associated with γ'' precipitation is present (double arrow) although less pronounced than for higher upper temperatures (see Fig. 7). On the contrary, both experiments with upper temperature at 980 °C showed no arrest related to γ'' precipitation during cooling. In fact, TEM observation of the sample held 10 min at 980 °C showed a distribution of γ'' much like the one in Fig. 10. This absence of fine and copious γ'' precipitation should be related, as already mentioned, to the sluggish dissolution process of these precipitates upon heating and holding at the upper temperature of the DTA cycle, but also to growth of the δ phase.

In the case of the sample heated up to 1000 °C and cooled at 10 °C/min after a 1 s holding, the SEM micrograph, such as the one presented in Fig. 13-A, shows a clear contrast between different grains. In the lighter zones, one can recognise the presence of large γ'' precipitates similar in size to the ones observed with TEM after heating at 980 °C (Fig. 10) while such large precipitates are not visible in the darker zones. TEM observation shows that the latter zones correspond to the presence of very small γ'' precipitates, like the microstructure observed after heating at 1100 °C (Fig. 8). The TEM image in Fig. 13-B illustrates the sharpness of the transition between these two types of microstructures, that were often found to correspond to a grain boundary (solid arrows in the figure). Fig. 13-C and -D respectively present details of the two types of microstructure. The small γ'' seem to be associated with globular δ precipitates, while the large ones coexist with

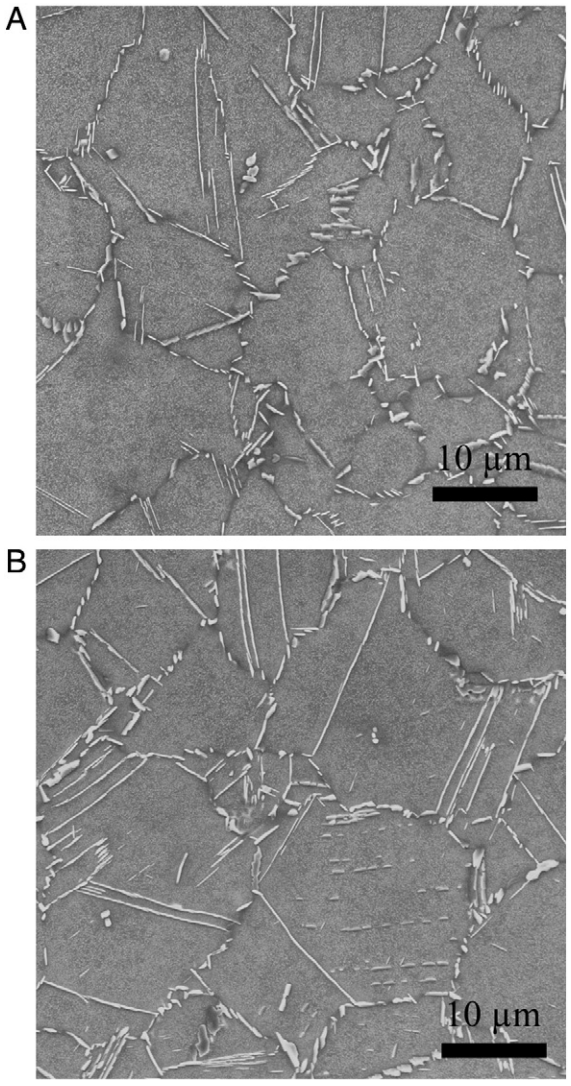

Fig. 12 – SEM micrograph (SE detector) of samples heated to 980 °C, hold 1 s (A) and 10 min (B) and then cooled at 10 °C/min.

intragranular acicular δ precipitates. This observation indicates that the γ'' phase does not dissolve in the same way in different places of the specimen.

4. Discussion

The above results suggest discussing three successive items: 1) solvus of the δ phase; 2) heterogeneities of precipitate dissolution upon heating the material close to the δ solvus; and 3) continuous cooling transformation diagrams.

4.1. *Solvus Temperature of δ Phase*

The value of the solvus of the alloy studied in this investigation, as determined by means of Fig. 4, is reported in Fig. 14 where it is compared to the data from the literature [15–22]. Although the present result is in line with other data, the high scatter that this figure shows should be highlighted. It might be due to the various means used to evaluate the solvus.

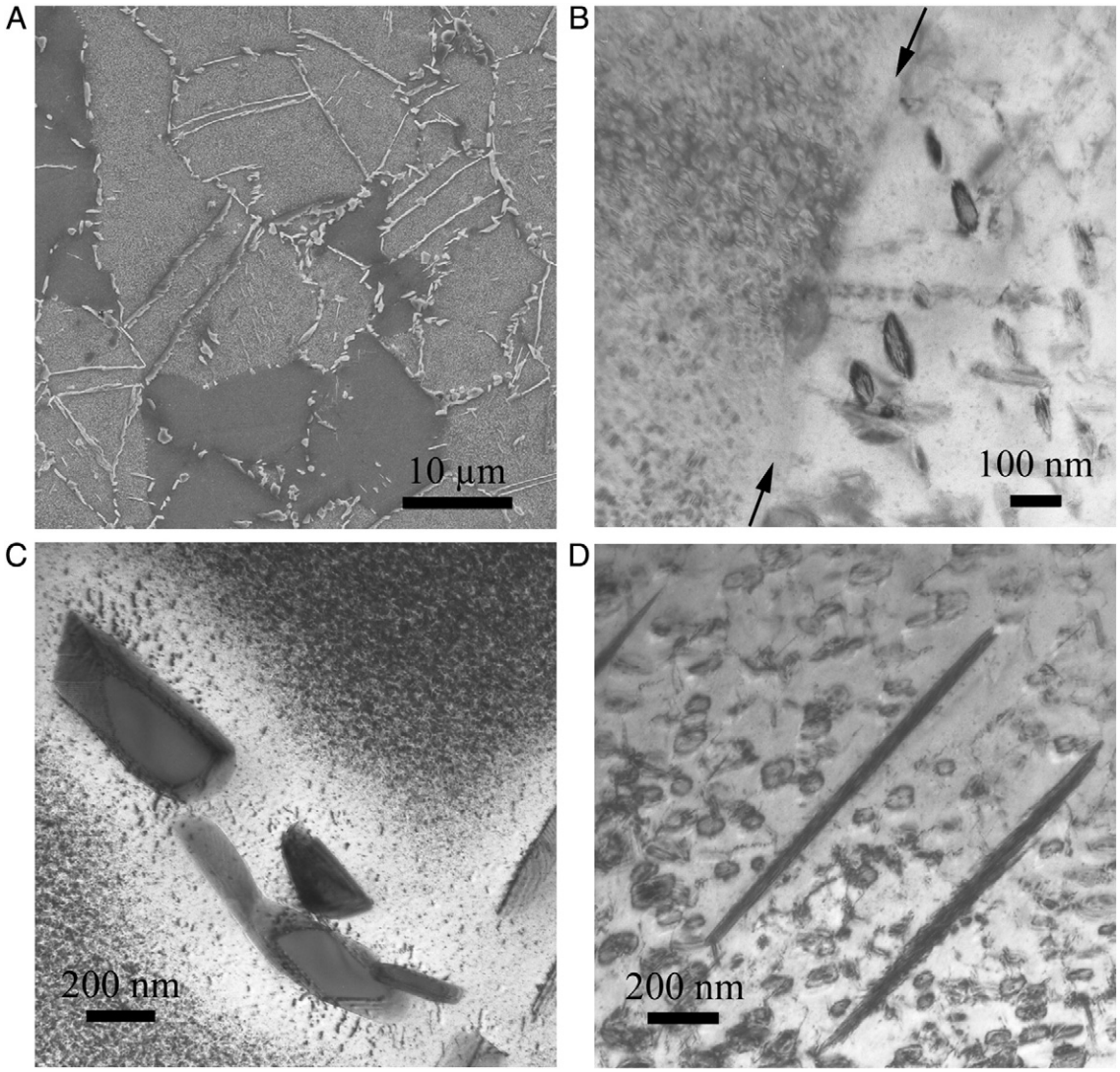

Fig. 13 – The microstructure of sample held 1 s at 1000 °C and then cooled at 10 °C/min is observed by SEM (SE detector) (A) and TEM (B–D). The TEM images show the abrupt transition between two types of γ″ precipitation in two adjacent grains (the grain boundary is indicated by the arrows — B) and details of the types of microstructure corresponding to small γ″ and globular δ (C) and large γ″ with δ plates (D).

4.2. *Heterogeneities in the Dissolution Process of the γ″ Phase*

Slama et al. [13] used dilatometry and DTA to study the dissolution process of the δ phase upon heating showing that it starts at 960 °C for a solvus estimated at 990 °C. By rapid heating to 990 °C and recording the dilatometric signal, it was concluded that most of the δ dissolution proceeds within the first 10 min of holding. The present results are very much in line with these conclusions: the dissolution of the γ'' phase which precipitated during heating of the AR material certainly interacts with precipitation and the dissolution of the δ phase for upper temperatures in the 960 to 1020 °C range. In particular, it has been established that γ'' precipitates may be retained in the matrix for quite a long time at temperatures well above their (metastable) solvus, and this is the reason for the interaction with the transformation process of the stable δ phase. The most striking result is that the kinetics of the dissolution process may vary from one grain to another. This heterogeneity could be related to the initial microstructure of the sample that is only partly recrystallised as seen in Fig. 2, which in turn may be connected to variations in local chemical composition inherited from the solidification process.

4.3. *CCT Diagram*

Garcia et al. [12] reported three CCT diagrams obtained by dilatometric analysis during cooling after holding the material at 1180 °C for 24, 72 and 90 hours. All of these diagrams show successive precipitation of Laves, δ, MC, γ'' and γ' with decreasing temperature. The temperature reported for the start of δ precipitation appears, however, quite high at more than 1100 °C. The authors emphasized that the corresponding CCT curves are shifted to longer times as the duration of the initial holding is increased, and suggested this to be due to a decrease in Nb supersaturation at grain boundaries. After holding 24 h at 1180 °C, the critical cooling rate for δ, γ' and γ''

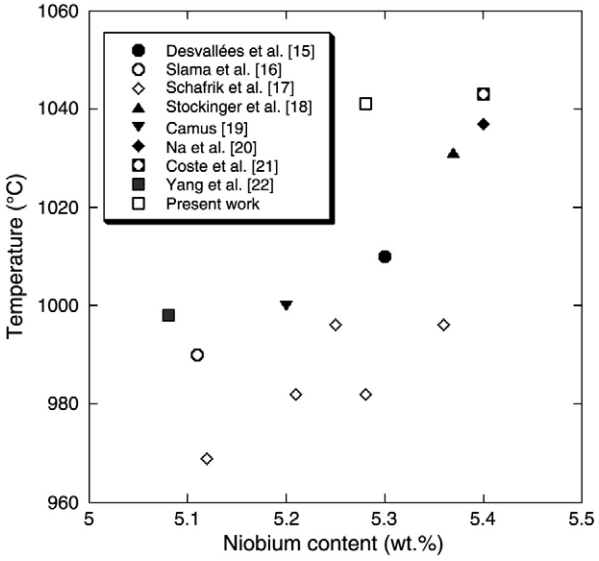

Fig. 14 – Delta solvus as function of the nominal niobium content of the alloys.

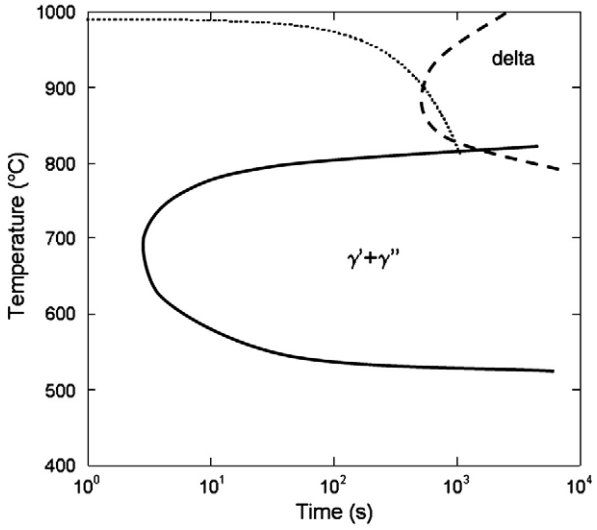

Fig. 15 – CCT curve (solid line) of alloy 718 according to Slama and Cizeron [Sla97b], cooling schedule of an alloy cooled at 10 °C/min from 990 °C (dotted line) and tentative CCT curve for δ phase from the present results (interrupted line).

precipitation, i.e. the cooling rate below which these phases will certainly precipitate, is about 600 °C/min. This critical cooling rate appears much higher than the value given by Geng et al. [14] who made microstructure investigations on material cooled from 1100 °C at rates in the range 0.1 to 20 °C/min, as well as on air, oil and water quenched samples. These authors found that no precipitation occurs at rates greater than 20 °C/min, or at least that precipitates were too small to be seen by TEM in those cases. At rates lower or equal to 20 °C/min, precipitation of γ'' was observed, and δ appeared when the cooling rate was further decreased below 5 °C/min. The present results are quite in line with these conclusions.

Slama and Cizeron [16] also used a dilatometer to follow precipitation during cooling (at rates in the 0.08 to 150 °C/s range) after a 15 min holding at 990 °C that was intended to dissolve all δ phases. They then systematically characterized the samples by TEM. In contrast with the work by Garcia et al. [12], they reported only one CCT curve for precipitation that is reproduced in Fig. 15 with a solid line, with the upper and lower parts of the curve relating to the beginning and the end of the transformation respectively. These authors found δ precipitates at all the cooling rates investigated, while TEM could detect a few small precipitates of γ' or γ'' only at cooling rates higher than 5 °C/s. The fact that δ is reported by Slama and Cizeron [16] to also precipitate at high cooling rates and at such a low temperature is doubtful in view of the TTT diagram (Fig. 1) and of the results by Geng et al. [14]. One may suggest that the δ precipitates they observed after such coolings were in fact already present at the start of cooling, and that the slope change recorded on the dilatometric curves was due to precipitation of γ'' and/or γ' in every case. The CCT curve from this work has been labelled accordingly in Fig. 15. In turn, the results by Slama and Cizeron show that detection of δ precipitation is difficult when the starting temperature is close to the solvus of that phase, in agreement with the present work. However, careful selection of the upper temperature and holding time was found here to allow for recording of an arrest associated with the growth of this phase. Namely, starting from 980 °C or 1000 °C and cooling down at 10 °C/min showed that precipitation of δ leads to a peak starting at 910 °C and ending at about 810 °C. This cooling schedule is reported in Fig. 15 with a starting temperature set in between 980 °C and 1000 °C at 990 °C (dotted line) and was used to draw a tentative CCT curve for δ growth when pre-existing precipitates exist. This CCT curve is shifted to much longer times with respect to γ' and γ'' precipitation.

5. Conclusion

Upon heating alloy 718 to forging temperature, dissolution kinetics of γ'' and δ phases appear quite sluggish. Furthermore, at temperatures a few tens of degrees below the δ solvus, the dissolution process of γ'' phase does not proceed at the same rate in every grain of the material and interacts with precipitation and dissolution of the δ phase. Stable or metastable precipitation after heating to process temperature may not be observed by DTA for every initial condition, but can be in some particular and useful conditions. This capacity will be used to investigate the competitive growth of δ and γ'' phases in alloy 718 at intermediate temperatures that are of interest for the forging process.

REFERENCES

[1] Paulonis DF, Oblak JM, Duvall DS. Precipitation in nickel-base alloy 718. Trans ASM 1969;62:611–22.
[2] Kirman I, Warrington DH. The precipitation kinetics of Ni_3Nb phases in a Ni–Fe–Cr–Nb alloy. Metall Trans 1970;1:2667–75.
[3] Oradei-Basile A, Radavich JF. A current TTT diagram for wrought alloy 718. In: Loria EA, editor. Superalloys 718, 625 and various derivatives. TMS; 1991. p. 325–35.

[4] Brooks JW, Bridge PJ. Metallurgical stability of Inconel alloy 718. In: Reicman S, et al, editor. Superalloys 1988. TMS; 1988. p. 33–42.
[5] Han YF, Deb P, Chatuverdi MC. Coarsening behaviour of γ' and γ'' particles in Inconel alloy 718. Metal Sci 1982;16: 555–61.
[6] Marsh AE. Aerospace forgings — materials, processes, products. Metallurgia January 1982:10–20.
[7] Slama C, Abdellaoui M. Structural characterization of the aged Inconel 718. J Alloy Comp 2000;306:277–84.
[8] Sundararaman M, Mukhopadhayay P, Banerjee S. Precipitation and room temperature deformation behaviour of Inconel 718. In: Loria EA, editor. Superalloys 718, 625, 706 and various derivatives. TMS; 1994. p. 419–40.
[9] Beaubois V, Huez J, Coste S, Brucelle O, Lacaze J. Short term precipitation kinetics of delta phase in strain free Inconel 718 alloy. Mater Sci Technol 2004;20:1019–26.
[10] Sundararaman M, Mukhopadhyay P, Barnejee S. Precipitation of the delta-Ni_3Nb phase in two nickel base superalloys. Metall Trans A 1988;19:453–65.
[11] Garcia CI, Camus DE, Loria EA, DeArdo AJ. Microstuctural refinement of as-cast alloy 718 via thermomechanical processing. In: Loria EA, editor. Superalloys 718, 625 and various derivatives. TMS; 1991. p. 925–39.
[12] Garcia CI, Lis AK, Loria EA, DeArdo AJ. Thermomechanical process and continuous cooling transformation behavior of IN-718. In: Antolovich SD, Stusrud RW, MacKay RA, Anton DL, Khan T, Kissinger RD, Klarstrom DL, editors. Superalloys 1992; 1992. p. 527–36.
[13] Slama C, Servant C, Cizeron G. Ageing of the Inconel 718 alloy between 500 and 750 °C. J Mater Res 1997;12:2298–316.
[14] Geng L, Na YS. Nho-Kwang Park, Continuous cooling 535 transformation behavior of alloy 718. Mater Lett 1997;30:401–5.
[15] Desvallées Y, Bouzidi M, Bois F, Beaude N. Delta phase in Inconel 718: mechanical properties and forging requirements. In: Loria EA, editor. Superalloys 718, 625, 706 and various derivatives. TMS; 1991. p. 337–50.
[16] Slama C, Cizeron G. Etude du comportement structural de l'alliage NC19FeNb (Inconel 718). J Phys III France 1997;7: 665–88.
[17] Schafrik RE, Ward DD, Groh JR. Application of alloy 718 in GE aircraft engines: past, present and next five years. In: Loria EA, editor. Superalloys 718, 625, 706 and various derivatives. TMS; 2001. p. 1–11.
[18] Stockinger M, Kozeschnik E, Buchmayr B, Horvath W. Modelling of delta-phase dissolution during preheating of Inconel 718 turbine disks. In: Loria EA, editor. Superalloys 718, 625, 706 and various derivatives. TMS; 2001. p. 141–8.
[19] Camus G. Traitements thermomécaniques de l'alliage NC19FeNb (Inconel 718) pour différentes applications sur turbomachines industrielles et aéronautiques, Thèse de doctorat, Institut National Polytechnique de Toulouse, 1986.
[20] Na YS, Yeom JT, Park NK, Lee JY. Simulation of microstructures for alloy 718 blade forging using 3D FEM simulator. J Mater Process Technol 2003;141:337–42.
[21] Coste S, Andrieu E, Huez J. Effect of heterogeneous distribution of particles on the formation of banded grain structure in wrought Alloy 718. Mater Sci Eng A 2005;396:92–8.
[22] Yang L, Chang K-M, Mannan S, De Barbadillo J. A new approach for verifying precipitate solvus in Inconel alloy 718. In: Loria EA, editor. Superalloys 718, 625, 706 and various derivatives. TMS; 1997. p. 353–65.